Clim. Past, 5, 537–550, 2009
www.clim-past.net/5/537/2009/


Climate of the Past

# Glacial-interglacial atmospheric $CO_2$ change: a possible "standing volume" effect on deep-ocean carbon sequestration

**L. C. Skinner**

Godwin Laboratory for Palaeoclimate Research, Dept. of Earth Sciences, Univ. of Cambridge, Cambridge, CB2 3EQ, UK

Received: 8 April 2009 – Published in Clim. Past Discuss.: 4 May 2009
Revised: 1 August 2009 – Accepted: 4 September 2009 – Published: 30 September 2009

**Abstract.** So far, the exploration of possible mechanisms for glacial atmospheric $CO_2$ drawdown and marine carbon sequestration has tended to focus on dynamic or kinetic processes (i.e. variable mixing-, equilibration- or export rates). Here an attempt is made to underline instead the possible importance of changes in the standing volumes of intra-oceanic carbon reservoirs (i.e. different water-masses) in influencing the total marine carbon inventory. By way of illustration, a simple mechanism is proposed for enhancing the marine carbon inventory via an increase in the volume of relatively cold and carbon-enriched deep water, analogous to modern Lower Circumpolar Deep Water (LCDW), filling the ocean basins. A set of simple box-model experiments confirm the expectation that a deep sea dominated by an expanded LCDW-like watermass holds more $CO_2$, without any pre-imposed changes in ocean overturning rate, biological export or ocean-atmosphere exchange. The magnitude of this "standing volume effect" (which operates by boosting the solubility- and biological pumps) might be as large as the contributions that have previously been attributed to carbonate compensation, terrestrial biosphere reduction or ocean fertilisation for example. By providing a means of not only enhancing but also driving changes in the efficiency of the biological- and solubility pumps, this standing volume mechanism may help to reduce the amount of glacial-interglacial $CO_2$ change that remains to be explained by other mechanisms that are difficult to assess in the geological archive, such as reduced mass transport or mixing rates in particular. This in turn could help narrow the search for forcing conditions capable of pushing the global carbon cycle between glacial and interglacial modes.

*Correspondence to:* L. C. Skinner
(luke00@esc.cam.ac.uk)

## 1 Explaining glacial-interglacial $CO_2$ change

Although it is clear that changes in atmospheric $CO_2$ have remained tightly coupled with global climate change throughout the past ∼730 000 years at least (Siegenthaler et al., 2005), the mechanisms responsible for pacing and moderating $CO_2$ change remain to be proven. The magnitude of the marine carbon reservoir, and its inevitable response to changes in atmospheric $CO_2$ (Broecker, 1982a), guarantees a significant role for the ocean in glacial-interglacial $CO_2$ change. Based on thermodynamic considerations, glacial atmospheric $CO_2$ would be reduced by ∼30 ppm simply due to the increased solubility of $CO_2$ in a colder glacial ocean (Sigman and Boyle, 2000); however this reduction would be counteracted by the reduced solubility of $CO_2$ in a more saline glacial ocean and by a large reduction in the terrestrial biosphere under glacial conditions (Broecker and Peng, 1989; Sigman and Boyle, 2000). The bulk of the glacial-interglacial $CO_2$ change therefore remains to be explained by more complex inter-reservoir exchange mechanisms, and the most viable proposals involve either the biological- or the physical "carbon pumps" of the ocean. On this basis, any mechanism that is invoked to explain glacial-interglacial $CO_2$ change must involve changes in the sequestration of $CO_2$ in the deepest marine reservoir (Broecker, 1982a; Boyle, 1988a, 1992; Broecker and Peng, 1989).

To date, three main types of conceptual model have been advanced in order to explain glacial-interglacial atmospheric $CO_2$ change: (1) those involving an increase in the export rate of organic carbon to the deep sea, either via increased nutrient availability at low latitudes or via increased efficiency of nutrient usage at high latitudes (Broecker, 1982a, b; Knox and McElroy, 1984); (2) those involving a reduction in the "ventilation" of water exported to the deep Southern Ocean (Siegenthaler and Wenk, 1984; Toggweiler and Sarmiento, 1985), either via sea-ice "capping" (Keeling and Stephens, 2001) or a change in the surface-to-deep mixing rate/efficiency (Toggweiler, 1999; Gildor and Tziperman,

Published by Copernicus Publications on behalf of the European Geosciences Union.

2001; Watson and Naveira Garabato, 2006); and (3) those involving changes in whole ocean chemistry and "carbonate compensation", possibly promoted by changes in the ratio of organic carbon and carbonate fluxes to the deep sea. (Archer and Maier-Reimer, 1994). Each of these conceptual models has its own set of difficulties in explaining the pattern and magnitude of past glacial-interglacial $CO_2$ change, and in fact none is likely to have operated in complete isolation (Archer et al., 2000; Sigman and Boyle, 2000). Nevertheless, one aspect of all of the proposed models that emerges as being fundamental to any mechanism proposing to explain glacial-interglacial $CO_2$ change is the balance between biological carbon export from the surface-ocean and the return of carbon to the surface by the ocean's overturning circulation. These two processes, one biological and one physical, essentially determine the balance of carbon input to and output from (and therefore the carbon content of) the deepest marine reservoirs (Toggweiler et al., 2003).

The regions of deep-water formation in the North Atlantic and especially in the Southern Ocean play a key role in setting the "physical side" of this balance. In the North Atlantic, carbon uptake via the "solubility pump" is enhanced by the large temperature change that surface water must undergo before being exported into the ocean interior. The formation of North Atlantic deep-water therefore represents an efficient mechanism for mixing $CO_2$ deep into the ocean interior (Sabine et al., 2004); though only to the extent that it is not completely compensated for (or indeed over-compensated for) by the eventual return flow of more carbon-enriched deep-water back to the surface (Toggweiler et al., 2003). Arguably, it is in controlling the extent to which the return flow of deep-water to the surface (which occurs primarily in the Southern Ocean) represents an effective 'reflux' of carbon to the atmosphere, acting against biological export, that the formation of deep-water in the Southern Ocean plays a pivotal role in controlling the partitioning of $CO_2$ between the surface- and the deep ocean. We might say that if the southern overturning loop "leaks" too much, it will be an efficient carbon source to the atmosphere (Toggweiler et al., 2003); and if it does not leak much, it will simply become a large standing carbon reservoir. The degree to which the southern overturning loop "leaks" depends on the efficiency of equilibration of up-welled Southern Ocean deep-water with the atmosphere, relative to the efficiency of carbon export (dissolved and particulate) from the surface Southern Ocean (Toggweiler, 1999; Gildor and Tziperman, 2001).

Today, a significant portion of the deep ocean (although not the deep Atlantic – "deep" meaning greater than $\sim$1 km in this context) is filled from the Southern Ocean by Lower Circumpolar Deep Water (LCDW) that is exported northwards into the various ocean basins from the eastward circulating Antarctic Circumpolar Current (ACC) (Orsi et al., 1999; Sloyan and Rintoul, 2001). This deep-water remains relatively poorly equilibrated with the atmosphere and is inefficiently stripped of its nutrients, thus maintaining an elevated "pre-formed" nutrient and dissolved inorganic carbon content. In part this is because of the very low temperature at which deep-water forms around Antarctica and because the rate of ocean – atmosphere $CO_2$ exchange cannot keep up with the rate of overturning in the uppermost Southern Ocean (Bard, 1988). However it is primarily because the bulk of southern sourced deep- and bottom-water is either produced via a combination of brine rejection below sea-ice and entrainment from the sub-surface, or converted from "aged" northern-sourced deep-waters that feed into the Southern Ocean via Upper Circumpolar Deep Water (UCDW) (Orsi et al., 1999; Speer et al., 2000; Webb and Suginohara, 2001; Sloyan and Rintoul, 2001). Intense turbulent mixing around topographic features in the deep Southern Ocean helps to enhance the amount of "carbon rich" subsurface water that is incorporated into LCDW (from UCDW above and from Antarctic Bottom Water, AABW, below), and that is subsequently exported northwards to the Atlantic and Indo-Pacific (Orsi et al., 1999; Naviera Garabato et al., 2004). The process of Lower Circumpolar Deep Water export in the deep Southern Ocean (as distinct from deep-water formation in the North Atlantic, and the vertical mixing in the uppermost Southern Ocean) can therefore be viewed as a mechanism that helps to "recycle" carbon-rich water within the ocean interior, circumventing ocean – atmosphere exchange, and eventual $CO_2$ leakage to the atmosphere.

It is notable that nearly all of the "physical pump" mechanisms that have been proposed as significant controls on glacial-interglacial $CO_2$ change have referred to dynamical (export- or mixing *rate*) or kinetic (ocean – atmosphere exchange *rate*) effects (e.g. Kohler et al., 2005; Toggweiler, 1999; Tziperman and Gildor, 2003; Brovkin et al., 2007; Peacock et al., 2006; Sigman and Haug, 2003). Consideration of the effect on atmospheric $CO_2$ of changes in the geometry, and therefore the *volumes*, of different intra-oceanic carbon reservoirs (i.e. different deep-water "masses") has largely escaped explicit treatment. This is surprising, given that the residence time of a reservoir will scale inversely to its renewal rate or positively to its volume. It is also surprising from an "experimental" perspective, given that most of the palaeoceanographic evidence available to us can tell us something about changes in water-mass distribution (hence volume), but usually cannot tell us much about changes in circulation or mixing rates. Furthermore, if we consider what controls the energy and buoyancy budgets of the ocean (and hence the capacity to maintain an overturning circulation), it is not obvious that the net overturning *rate* of the ocean must have been significantly different from modern over long time periods in the past (Gordon, 1996; Wunsch, 2003) – even if it is true that the reconstructed hydrography of the glacial ocean is inconsistent with the modern circulation (especially in terms of vertical property distributions) (Marchal and Curry, 2008). The circulation rate (mass transport) of the glacial ocean therefore remains poorly constrained, despite well-defined property distribution (hence inventory) changes.

The purpose of the present study is to focus attention on the importance of distinguishing between past changes in the distribution of water-masses (which we can know something about) and past changes in their renewal rates (which we tend to know very little about), in particular when considering the role of the ocean circulation in setting the marine carbon inventory. By way of illustration, the simple hypothesis is advanced that the amount of carbon that can be "bottled up" in the deep ocean may be significantly affected by changes in the *volumes* of different glacial deep-water masses, prior to any imposed changes in overturning-, gas exchange- or biological export *rates* (but including the effects of any redistribution of temperature, salinity, and pre-formed/remineralised nutrients that is incurred). Of course, the suggestion is not that changes in circulation- or export rates are unimportant; but rather that they are not exclusively important. The distinction between these two aspects of the ocean circulation (i.e. water-mass distribution *versus* overturning rate), and the evaluation of their individual impacts on atmospheric $CO_2$, could prove to be important in assessing the mechanisms of glacial-interglacial $CO_2$ change, in particular if it is possible for these two aspects of the ocean circulation to become decoupled, for example on long time-scales or for specific forcing. Put another way: if the mechanisms or time-scales required to alter the marine carbon inventory via changes in overturning rates and water-mass volumes differ, then they cannot be usefully conflated in the single term "ocean circulation" when considering the causes of glacial-interglacial $CO_2$ change.

In this paper additional emphasis is placed on how the hypsometry of the ocean basins (the area distribution at different water depths) may affect the efficiency of volumetric water-mass changes that are caused by the shoaling/deepening of water-mass mixing boundaries. A notable fact in this regard is that ∼56% of the sea-floor lies between 6000 and 3000 m (Menard and Smith, 1966), thus accounting for a majority increment in the ocean's volume. If a water mass that once occupied the >5 km interval in the Atlantic comes to occupy the >2 km interval, it will have increased its volume in this basin almost four-fold.

## 2 A thought experiment: a "southern flavour ocean"

Arguably, one of the least ambiguous aspects of the palaeoclimate archive is the record of glacial-interglacial change in $\delta^{13}C$ recorded by benthic foraminifera from the Atlantic Ocean (Curry and Oppo, 2005; Duplessy et al., 1988). The data suggest, at the Last Glacial Maximum, a more positive $\delta^{13}C$ of DIC in the upper ∼2 km of the Atlantic, and a more negative $\delta^{13}C$ of dissolved inorganic carbon (DIC) below this in the deepest Atlantic. These data do not appear to be consistent with the modern water-mass geometry/circulation (Marchal and Curry, 2008). The most widespread and well-supported interpretation of these data is that they represent a redistribution of glacial northern- and southern-sourced deep and intermediate water-masses, including in particular an incursion of glacial southern-sourced deep water (rich in preformed and remineralised nutrients, and of low $\delta^{13}C$) into the deep North Atlantic, up to a water depth of ∼2–3 km (Curry et al., 1988; Duplessy et al., 1988; Oppo and Fairbanks, 1990; Oppo et al., 1990; Boyle, 1992; Curry and Oppo, 2005; Hodell et al., 2003). This interpretation is now strongly supported by glacial Atlantic benthic foraminiferal Cd/Ca, Zn/Ca and B/Ca ratios (Marchitto and Broecker, 2005; Boyle, 1992; Keigwin and Lehmann, 1994; Marchitto et al., 2002; Yu and Elderfield, 2007). Auxiliary support has been provided by benthic radiocarbon measurements from the North Atlantic (Robinson et al., 2005; Skinner and Shackleton, 2004; Keigwin, 2004), and neodymium isotope measurements ($\varepsilon_{Nd}$) from the South Atlantic (Rutberg et al., 2000; Piotrowski et al., 2005, 2004). An elegant box-model investigation of the possible causes of glacial deep-ocean chemistry (Michel et al., 1995) and coupled atmosphere-ocean general circulation model (AOGCM) simulations of the "last glacial maximum" circulation (e.g. Shin et al., 2003; Kim et al., 2003) have also added weight to this interpretation of glacial deep-water mass geometry. If we assume that the relationships between deep-water radiocarbon activity, carbonate ion concentration, $\delta^{13}C$ of DIC and $TCO_2$ remained similar between glacial and interglacial (pre-industrial) times, at least for deep-water exported northwards from the Southern Ocean, then we may also infer that the water that apparently replaced NADW in the Atlantic and dominated LCDW export to the Indo-Pacific basins was also of relatively high $TCO_2$. Indeed, radiocarbon evidence (Marchitto et al., 2007), dissolution indices (Barker et al., 2009), benthic $\delta^{13}C$ (Ninneman and Charles, 2002; Hodell et al., 2003) and pore-water temperature/salinity estimates (Adkins et al., 2002) all tend to suggest that deep-water exported from the Southern Ocean during the last glacial would have represented a concentrated and isolated carbon reservoir that was very poorly equilibrated with the atmosphere.

Given these constraints on the deep-water hydrography near the height of the last glaciation (Lynch-Steiglitz et al., 2007), one question immediately arises: how much must the *volume* of southern-sourced deep-water (LCDW) have increased, regardless of its export *rate*, in order to accomplish the observed change (i.e. filling the deep Atlantic, and dominating the deep-water export to the Indian and Pacific basins)? Further, and more importantly, what would have been the immediate effect on deep-water $CO_2$ sequestration, if any, of the resulting redistribution of dissolved inorganic carbon, nutrients and temperature/salinity? Answering the first question is straightforward enough: as noted above, based on the hypsometry of the Atlantic basin (Menard and Smith, 1966), raising the upper boundary of southern-sourced deep-water (assumed for the sake of argument to be approximately flat) from 5 km to 2.5 km in the Atlantic requires this water-mass to increase its Atlantic volume from

under 20 million km$^3$ to nearly 70 million km$^3$ (just under a 4-fold increase). In order to determine the eventual impact of this volumetric change on the carbon-storage capacity of the ocean we would obviously require knowledge of the changing chemistry of the various deep-water masses in the ocean as well as their turnover and "ventilation" (atmosphere equilibration) rates, and the flux of dissolved carbon that they eventually incorporate via biological export. However, if we assume simplistically that nothing in the ocean changes except the volume occupied by southern-sourced deep-water (i.e. the chemistry of all water-masses stays the same, but not their volumetric contribution to the ocean's total budget), then we can infer that for a 4-fold increase in the volume of AABW at the expense of NADW (having average total dissolved $CO_2$ concentrations of $\sim$2280 $\mu$mol kg$^{-1}$ and $\sim$2180 $\mu$mol kg$^{-1}$, respectively, Broecker and Peng, 1989) the ocean would need to gain $\sim$63 Gt of carbon. If we assume that all this carbon must come from the atmosphere, then atmospheric $pCO_2$ would have to drop by $\sim$30 ppm, given 1 ppm change per 2.12 Gt carbon removed from the atmosphere (Denman et al., 2007). This is equivalent to $\sim$38% of the total observed glacial-interglacial $CO_2$ change (Siegenthaler et al., 2005), and is comparable to the magnitude of atmospheric $CO_2$ changes that are likely to have arisen from other viable mechanisms such as biological export increase, or carbonate compensation (Peacock et al., 2006).

Clearly many of the assumptions made in the above thought experiment might not be valid: the chemistry and dynamics, not to mention the character and rate of biological export, of the glacial ocean will probably not have remained constant. Nevertheless, palaeoceanographic proxy evidence holds that the basic premise of the thought experiment is valid: the volume of deep water closely resembling modern southern-sourced deep-water apparently increased significantly during the last glaciation. It seems warranted therefore to evaluate the impacts of this premise in a slightly more sophisticated way. The question to be answered is: does a deep ocean dominated by a LCDW-like water-mass hold more carbon at steady state (on time-scales longer than the mixing time of the ocean)? Below, a very simple box model is used as a first step toward answering this question.

## 3 Box-model description

Figure 1 illustrates a simple box-model that has been constructed in order to explore in more detail the implications of deep-water mass geometry (*versus* overturning rate) changes for glacial-interglacial $CO_2$ variability. This model comprises an atmosphere and six ocean boxes (Southern Ocean, low-latitude, North Atlantic, northern deep water, intermediate-water and southern deep water), and involves two coupled circulation cells with down welling in the southern and northern high latitudes. Geological exchange of minerals and nutrients (river alkalinity input, sedimentation, carbonate compensation) is not included in this model. Particle fluxes are treated as directly exported dissolved matter, with carbon and phosphate being exported in fixed proportions, as defined by modified Redfield Ratios (C:N:P:$O_2$=130:16:1:-169) (Toggweiler and Sarmiento, 1985), and carbonate being exported in fixed proportion to the $TCO_2$ of the water. Particle fluxes are diagnosed for a baseline "pre-industrial" box-model scenario according to observed phosphate concentrations in the modern ocean (Najjar et al., 1992):

$$P = \frac{C^*}{P^*}\left(\frac{([PO_4] - [PO_4]_{\mathrm{mod}})V}{\tau}\right)$$

where $P$ is the instantaneous organic carbon flux, $C^*/P^*$ is the ratio of organic carbon to phosphate in the particulate matter, $V$ is the box volume, $\tau$ is the restoring time-scale (set to 0.1 year), and $[PO_4]$ and $[PO_4]_{\mathrm{mod}}$ are the instantaneous and restoring phosphate concentrations, respectively. In subsequent "altered" box-model scenarios, particle fluxes vary according to "Michaelis-Menton" type dynamics (Dugdale, 1967), with less export being supported by lower nutrient concentrations. This removes the possibility of unrealistically high/low export productivity for very low/high nutrient levels respectively:

$$P = \frac{C^*}{P^*}\left(\frac{\omega[PO_4]}{k_m + [PO_4]}\right)$$

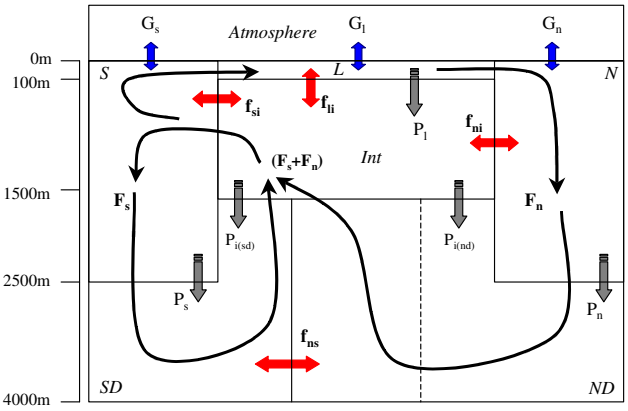


**Fig. 1.** Box-model schematic (S, southern surface; L, low-latitude surface; N, northern surface; ND, north deep; Int, intermediate; SD, south deep). The vertical dashed line is intended to suggest an alternative hypothetical box geometry, where southern sourced water dominates the deep ocean. Heavy black lines indicate thermohaline circulation (Fn=northern overturning; Fs=southern overturning). Red arrows indicate two-way exchange (i.e. mixing) terms. Blue arrows indicate gas exchange. Grey arrows indicate particle fluxes. The particle fluxes Pi(sd) and Pi(nd) that by-pass the intermediate box from the low-latitude box are calculated in proportion to the volume of each deep box relative to the total deep ocean in the model, such that if Vnd/Vd=f, Pi(nd)=f$\times$0.1$\times$Pl and Pi(sd)=(1-f)$\times$0.1$\times$Pl. Approximate box depths are indicated at left (surface areas are given in Table 1).

In the above equation, $k_m$ is set to $2.5\,e^{-4}$ mol m$^{-3}$ (Schulz et al., 2001), and $\omega$ (the biological uptake rate) is diagnosed from the equilibrium conditions for the "modern box-model scenario" (preceding equation).

The calculated components of the model include phosphate, alkalinity, total dissolved $CO_2$ ($TCO_2$), carbonate ion ($CO_3^{2-}$), $pCO_2$, apparent oxygen utilisation (AOU) and normalised radiocarbon concentration ($\Delta^{14}C$). Because the modelled radiocarbon concentrations are not normalised with respect to $\delta^{13}C$, $\Delta^{14}C$ reported here is actually equivalent to $d^{14}C$ by definition (Stuiver and Polach, 1977). Idealised mass-balance equations for the evolution of box concentrations are of the form:

$$V_n \frac{dC_n}{dt} = F_n(C_l - C_n) + f_{ni}(C_i - C_n) - P_n \frac{C^*}{P^*} + F_{AO}$$

(e.g. northern surface box)

$$V_{sd} \frac{dC_{sd}}{dt} = F_s(C_s - C_{sd}) + f_{ns}(C_{nd} - C_{sd}) + (P_s + P_{i(sd)}) \frac{C^*}{P^*}$$

(e.g. southern deep box)

where $C$ indicates the box concentration, $F$ and $f$ indicate water fluxes, $P$ indicates particulate carbon fluxes (multiplied by chemical export/consumption ratios for different constituents, $C^*/P^*$) and $F_{AO}$ indicates an air-sea exchange term (applicable to carbon dioxide and radiocarbon). The deep boxes receive particle fluxes from the high northern/southern latitude surface boxes as well as the intermediate box, through which one tenth of the low latitude particulate flux is transmitted. Each deep box receives particulate flux from the intermediate box in proportion to its relative volume (see Fig. 1). Surface boxes have AOU set to zero.

For the calculation of the $TCO_2$ of the surface boxes, an extra exchange term with the atmosphere must be included:

$$V_s \frac{dC_s}{dt} =$$

$$F_s(C_i - C_s) + F_n(C_i - C_s) + f_{si}(C_i - C_s) - P_s \left( \frac{C}{C_{\text{org}}} \right)$$

$$+ (CO_2)_{\text{SOL-s}}$$

(e.g. southern surface box)

The air-sea gas exchange ($(CO_2)_{SOL}$) is defined according to the thermodynamics of Millero (1995) (Eqs. 26, 41 and 42 therein), and follows a similar scheme to that of Toggweiler and Sarmiento (1985), such that:

$$(CO_2)_{\text{SOL-s}} = \left[ (pCO_2)_s - (pCO_2)_{\text{atm}} \right] A_s g_s \alpha_s$$

where $A_s$ and $g_s$ are southern surface box area (m$^2$) and gas piston velocity (kg m$^{-2}$ yr$^{-1}$), respectively; $(pCO_2)_s$ and $(pCO_2)_{\text{atm}}$ are the partial pressures for $CO_2$ in the southern surface box and the atmosphere respectively, and where $\alpha_s$ is the southern surface box solubility coefficient for $CO_2$ (Millero, 1995).

The carbonate system is treated using the C-SYS calculation scheme of (Zeebe and Wolf-Gladrow, 2001) given alkalinity, $TCO_2$, pressure, temperature and salinity. The atmospheric $pCO_2$ is updated at each time step by integrating the air-sea $CO_2$ fluxes from each surface box:

$$V_{\text{atm}} \frac{d(pCO_2)_{\text{atm}}}{dt} = \left[ (pCO_2)_s - (pCO_2)_{\text{atm}} \right] A_s g_s \alpha_s +$$

$$+ \left[ (pCO_2)_l - (pCO_2)_{\text{atm}} \right] A_l g_l \alpha_l + \left[ (pCO_2)_n - (pCO_2)_{\text{atm}} \right] A_n g_n \alpha_n$$

For radiocarbon, an extra term is included in the equations to account for radioactive decay. Thus for the northern surface

**Table 1.** Input parameterisation for "baseline" model run. Only $R_{ns}$ is varied in subsequent model runs.

| Parameter | Label | Value | Source |
|---|---|---|---|
| *Fluxes* | | | |
| Northern overturning | $F_n$ | 28 Sv | – |
| Southern overturning | $F_s$ | 16.5 Sv | – |
| Low lat. vertical mixing | $f_{li}$ | 5 Sv | – |
| Northern high lat. vertical mixing | $f_{ni}$ | 10 Sv | – |
| Southern high lat. vertical mixing | $f_{si}$ | 10 Sv | – |
| Deep mixing | $f_{ns}$ | 5 Sv | – |
| *Volumes, Areas* | | | |
| Total ocean volume | $V_o$ | $1.3\times10^{18}$ m$^3$ | a |
| Total ocean area | $A_o$ | $3.5\times10^{14}$ m$^2$ | a |
| Mass of atmosphere | $V_{\text{atm}}$ | $1.773\times10^{20}$ mol | b |
| N. high lat. box area/Total area | $A_n/A_o$ | 0.07 | c |
| S. high lat. box area/Total area | $A_s/A_o$ | 0.17 | c |
| Vol. NDW/Vol. SDW | $R_{ns}$ | 1.43 | a (see text) |
| *Global inventories* | | | |
| Phosphate | $P_{\text{glob}}$ | $2.769\times10^{15}$ mol | b |
| Alkalinity | $Alk_{\text{glob}}$ | $3.12\times10^{18}$ mol | d |
| Total carbon inventory | $C_{\text{glob}}$ | $3.03\times10^{18}$ mol | d |
| Radiocarbon ($^{14}C$) | $^{14}C_{\text{glob}}$ | $3.01\times10^{6}$ mol | d |
| *Temperature, Salinity* | | | |
| Northern temperature | $T_n$ | 5°C | – |
| Southern temperature | $T_s$ | 1°C | – |
| Low lat. temperature | $T_l$ | 21.5°C | – |
| Northern salinity | $S_m$ | 35.0‰ | – |
| Southern salinity | $S_s$ | 34.7‰ | – |
| Low lat. salinity | $S_l$ | 36.0‰ | – |
| *Restoring phosphate* | | | |
| Southern $PO_4$ | $P_s$ | 1.9 $\mu$mol kg$^{-1}$ | e |
| Low lat. $PO_4$ | $P_l$ | 0.2 $\mu$mol kg$^{-1}$ | e |
| Northern $PO_4$ | $P_n$ | 0.5 $\mu$mol kg$^{-1}$ | e |
| Redfield Ratios | | | |
| Carbon/phosphate | C/P | 130 | b |
| Oxygen/phosphate | $O_2$/P | 138 | f |
| Southern $CaCO_3/TCO_2$ | S-Ca/$CO_2$ | 0.2 | g |
| Low lat. $CaCO_3/TCO_2$ | L-Ca/$CO_2$ | 0.2 | g |
| Northern $CaCO_3/TCO_2$ | N-Ca/$CO_2$ | 0.25 | g |

a – Menard and Smith (1966);
b – Toggweiler and Sarmiento (1985);
c – estimates for globe >50° S and 40% of >50° N;
d – Key et al. (2004), plus 596 Gt C in the atmosphere;
e – Garcia et al. (2006), Marchal et al. (1998); Najjar et al. (1992);
f – Redfield et al. (1962);
g – derived from Alk/P in reference b.

box, the mass balance equation for radiocarbon is:

$$V_n \frac{dC_n}{dt} = F_n(C_l - C_n) + f_{ni}(C_i - C_n) - P_n \frac{C^*}{P^*} + F_{AO} - \lambda C_n$$

Here $\lambda$ is the radiocarbon decay constant ($1.2097\,\mathrm{e}^{-4}\,\mathrm{yr}^{-1}$). Radiocarbon is transported as a concentration ($\mu\mathrm{mol\,kg}^{-1}$), such that the ratio of radiocarbon to total carbon ($R^{14}\mathrm{C}$) is determined by dividing the radiocarbon concentration by the total carbon concentration of the relevant box at each timestep. The normalised radiocarbon concentration is then determined as:

$$\Delta^{14}C_{\mathrm{box}} = \left( \frac{R^{14}C_{\mathrm{box}}}{R^{14}C_{\mathrm{std}}} - 1 \right) \times 1000$$

The radiocarbon concentrations of the various boxes are expressed relative to the pre-industrial standard $^{14}\mathrm{C/C}$ ratio of $1.176\,\mathrm{e}^{-12}$. Biological uptake/release of radiocarbon and cosmogenic radiocarbon production are not treated explicitly in this model. Instead these terms are diagnosed for an equilibrium atmospheric radiocarbon concentration equal to the pre-industrial standard ($^{14}\mathrm{C/C}$=$1.176\,\mathrm{e}^{-12}$). Once diagnosed, both terms are kept constant for experiments that involve modifications in box-model geometry. The global radiocarbon inventory is also fixed at its pre-industrial value, and can be maintained at this constant level once a pre-industrial equilibrium has been attained. Atmosphere – ocean exchange of radiocarbon is calculated as formulated for example by (Müller et al., 2006), such that:

$$F_{AO} = g A_o K_h \frac{p\mathrm{CO}_{2-\mathrm{atm}}}{\mathrm{TCO}_{2-\mathrm{o}}} \left( R^{14}C_{\mathrm{atm}} - R^{14}\mathrm{C_o} \right)$$

where $F_{AO}$ is the atmosphere to ocean radiocarbon flux, $g$ is the gas piston velocity (fixed at $3\,\mathrm{ms}^{-1}$), $A_o$ is the exposed ocean box area, $K_h$ is the $CO_2$ solubility constant for the ocean surface and subscripts $_{-\mathrm{atm}}$ and $_{-o}$ refer to atmospheric- and oceanic carbon concentrations or radiocarbon ratios.

A numerical integration method (ODE-45 in Matlab's Simulink) is used to update the box concentration at the end of each time step, until all boxes reach a steady equilibrium. In order for radiocarbon to reach equilibrium the model must be integrated for ∼20 000 model years. In the model, a correction scheme is used to check that the global inventories of phosphate, alkalinity and (radio-) carbon do not drift, and are all maintained at prescribed constant values. This correction scheme in fact only needs to be invoked for radiocarbon, since it is the only modelled species that includes diagnosed net input/output terms (production, decay and terrestrial biosphere uptake). Radiocarbon inventory correction factors thus differ from 1 during the "wind-up" to equilibrium, while the atmospheric input and output terms (cosmogenic production minus biosphere uptake) are being diagnosed. Note that box-volumes in the model do not change during simulations ($dV/dt$=0). It should also be noted that although the flow scheme of the box model essentially represents an Atlantic Ocean (i.e. it has two deep overturning "limbs"), it is scaled to global proportions so that the volumes and concentrations of the atmosphere and the ocean balance with global inventories (all of which are fixed input parameters). Nevertheless, the volumes of the two deep-water boxes are scaled relative to each other according to the hypothesised representation of North Atlantic and Antarctic deep-water end-members throughout the global ocean.

The model is initiated with the concentrations of all boxes set to the global average, except for the $p\mathrm{CO}_2$ of the surface boxes and the atmosphere, which are set arbitrarily close to zero (this avoids singularities in the calculation of initial radiocarbon concentrations). Equilibrium outcomes were not found to be sensitive to changes in these initial concentration conditions, since global inventories are maintained. In all model runs temperatures and salinities are also kept constant, in order to investigate exclusively the effect of water-mass geometry changes.

### 3.1 Model parameterisation and sensitivity

The parameterisation of the model's mass transport and mixing rate terms is outlined in Table 1. Circulation rates for the (modern) northern and southern overturning loops were initially set according to (Ganachaud and Wunsch, 2000). These export rates were then augmented in fixed proportion to each other (1:1.7) in order to achieve deep ocean radiocarbon concentrations that more closely matched the modern ocean (average deep-ocean age ∼1400 years) and such that atmospheric carbon dioxide reached an appropriate pre-industrial value (∼ 280 ppm) when restoring to modern surface phosphate concentration estimates (see below). Mixing rates between boxes were set arbitrarily to 10 Sv in the high latitudes and 5 Sv for the deep-ocean and the low-latitude surface ocean, where it can be argued that up-welling should be small compared to high-latitude overturning (Gnanadesikan et al., 2007). The sensitivity of the variable biological export was diagnosed by restoring to prescribed surface phosphate concentrations, as described above, once appropriate mass transport rates were estimated (see Table 1). With the net biological export to the deep boxes estimated to be ∼10% of export production at 100 m (Martin et al., 1987), the total biological export at 100 m in the baseline model run is $\sim 20\,\mathrm{PgC\,yr}^{-1}$. Although this value is rather high, there is ample scope for reducing it by prescribing a more sluggish net overturning rate in the model, while maintaining approximate pre-industrial atmospheric $p\mathrm{CO}_2$, and re-diagnosing (necessarily lower) biological uptake rates. As illustrated below, this can be done without significantly affecting the carbon and radiocarbon distributions in the model, and indeed without affecting the outcome of this study. Directly tuning the model to expected net biological export rates (closer to

$\sim$10 PgC yr$^{-1}$, Kohler et al., 2005) can therefore be safely avoided.

Figure 2 illustrates the sensitivity of modelled atmospheric $pCO_2$ and deep-ocean radiocarbon ventilation with respect to changes in the physical transport and mixing rate parameters. As expected, the parameter that most strongly constrains both the ocean – atmosphere radiocarbon- and $CO_2$ partitioning is the net overturning transport rate ($F_n$ + $F_s$, where $F_s$ = $F_n$/1.7; see Fig. 1). In the majority of the sensitivity tests illustrated in Fig. 2 (solid lines), biological "uptake rates" ($\omega$, the variable-export sensitivity) were maintained at the values diagnosed for the baseline "pre-industrial" scenario (i.e. for $F_n$=28 Sv, $F_s$=16.5 Sv, and for modern surface-ocean phosphate concentrations; see Table 1). However, when surface-ocean nutrient (phosphate) concentrations are restored to modern values while at the same time changing the mixing rate parameters, the impact of large changes in overturning rates on atmospheric $pCO_2$ is greatly reduced (crossed circles in Figure 2). This demonstrates how the balance between physical overturning and biological export effectively sets the carbon sequestration capacity of the deep ocean for a given deep-water geometry (e.g. Sarmiento and Toggweiler, 1984). It also illustrates that a lower net biological export could be obtained with a lower net overturning rate, while approximately maintaining pre-industrial $pCO_2$ and deep-ocean $\Delta^{14}C$.

Clearly, a box-model like the one presented here represents a highly conceptualised system, though in this case only radiocarbon (as a ventilation time-scale indicator), surface-ocean phosphate concentration (as a biological export rate indicator), and atmospheric $pCO_2$ (as a carbon climatology indicator) are used to "tune" the model. The rest of the box-model equilibrium chemistry is determined by these conditions, and can therefore be used for a first-order evaluation of the model behaviour. The "realism" of the baseline pre-industrial model scenario is illustrated in Fig. 3 relative to modern/pre-industrial observations (Key et al., 2004; Broecker and Peng, 1982). The modern/pre-industrial "observations" should be seen merely as indications of what plausible box concentrations might be, since their counterparts in reality are difficult to assess. The concentrations, volumes and chemical inventories of the boxes for the baseline control scenario are listed in Table 2. As shown in Fig. 3, even this highly simplified model is capable of mimicking the chemical distribution of the modern ocean with adequate realism, without being explicitly tuned to do so.

The goal will be to explore differences in the equilibrium carbon-sequestration capacity of the box-model ocean for a series of different deep-water box geometries. In order to do this, the model is run to equilibrium after the relative volumes of the two deep-water boxes in the model are changed, while the total volume is of course maintained and while the global chemical inventories and all other model parameters are kept constant.

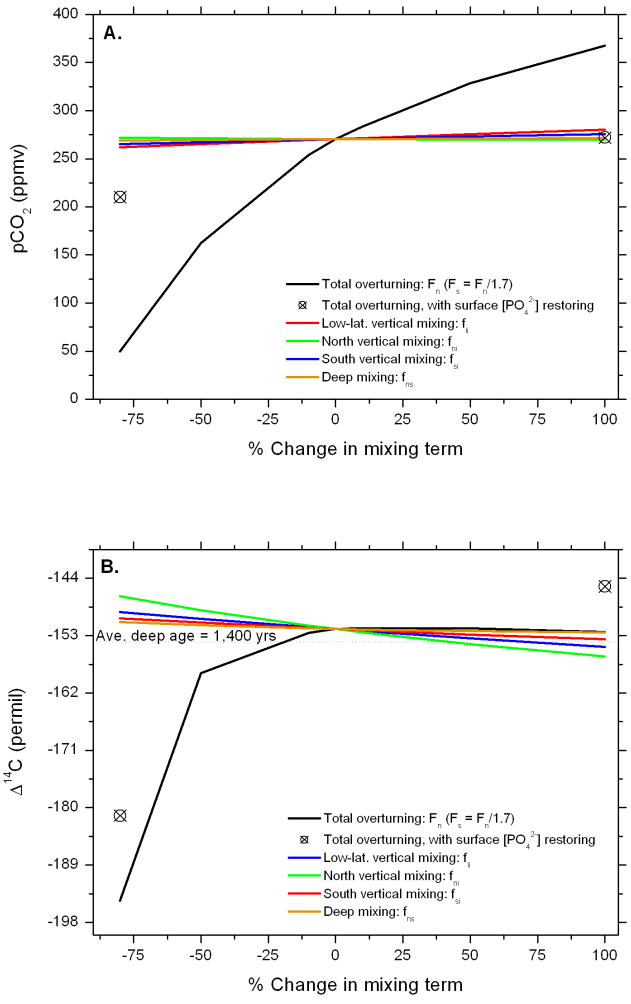


**Fig. 2.** Sensitivity of modelled atmospheric $pCO_2$ **(a)** and average deep ocean 14C **(b)** to changes in the box-model physical mixing terms, expressed here as percentages relative to the baseline values given in Table 1. The crossed circles indicate results for experiments where both the total overturning strength (Fn+Fs) and the surface-box biological uptake rates (i.e. export efficiency) were varied in order to maintain prescribed modern surface box phosphate concentrations.

## 4 Model experiments

As noted above, the reconstruction of past changes in the dynamical structure (flow rates) of the ocean remains a major challenge (Wunsch, 2003; Lynch-Steiglitz et al., 2007). However, proxies for past deep-water composition, such as for example benthic foraminiferal Cd/Ca (Boyle, 1988b), $\delta^{13}C$ (Duplessy et al., 1988; Curry and Oppo, 2005) and more recently dispersed ferromanganese oxide $\varepsilon_{Nd}$ (Goldstein and Hemming, 2003), more readily allow us to infer past changes in water-mass distribution. Thus during the last glacial in the Atlantic and the Atlantic sector of the Southern Ocean it would appear that NADW-influenced deep-water

**Table 2.** Box concentrations and inventories for "baseline" run ($R_{ns}$=1.43).

| $R_{ns}$=1.43 | | Box concentrations | | | | Box inventories | | | |
|---|---|---|---|---|---|---|---|---|---|
| Box | Box inventory ($10^{19}$ kg) | $TCO_2$ ($\mu$mol kg$^{-1}$) | Alkalinity ($\mu$mol kg$^{-1}$) | $\Delta^{14}C$ (‰) | Phosphate ($\mu$mol kg$^{-1}$) | $TCO_2$ (mol) | Alkalinity (mol) | $^{14}C$ (mol) | Phosphate (mol) |
| South high latitude | 1.523 | 2147 | 2310 | −133 | 1.98 | 3.269E+16 | 3.517E+16 | 3.33E+04 | 3.016E+13 |
| Low latitude | 2.725 | 1870 | 2223 | −6 | 0.21 | 5.096E+16 | 6.057E+16 | 5.96E+04 | 5.802E+12 |
| North high latitude | 0.627 | 2001 | 2233 | −70 | 0.53 | 1.254E+16 | 1.400E+16 | 1.37E+04 | 3.302E+12 |
| North deep | 52.44 | 2111 | 2275 | −119 | 1.25 | 1.107E+18 | 1.193E+18 | 1.15E+06 | 6.560E+14 |
| Intermediate depth | 40.87 | 2265 | 2330 | −178 | 2.40 | 9.258E+17 | 9.522E+17 | 8.95E+05 | 9.792E+14 |
| South deep | 36.67 | 2327 | 2359 | −200 | 2.99 | 8.534E+17 | 8.650E+17 | 8.03E+05 | 1.095E+15 |
| Atmosphere | 1.77E+20 (mol) | 270 (ppm) | | 0.04708 | | 4.794E+16 | | 5.64E+04 | |
| | | | | | Total inventories: | 3.03E+18 | 3.12E+18 | 3.01E+06 | 2.769E+15 |

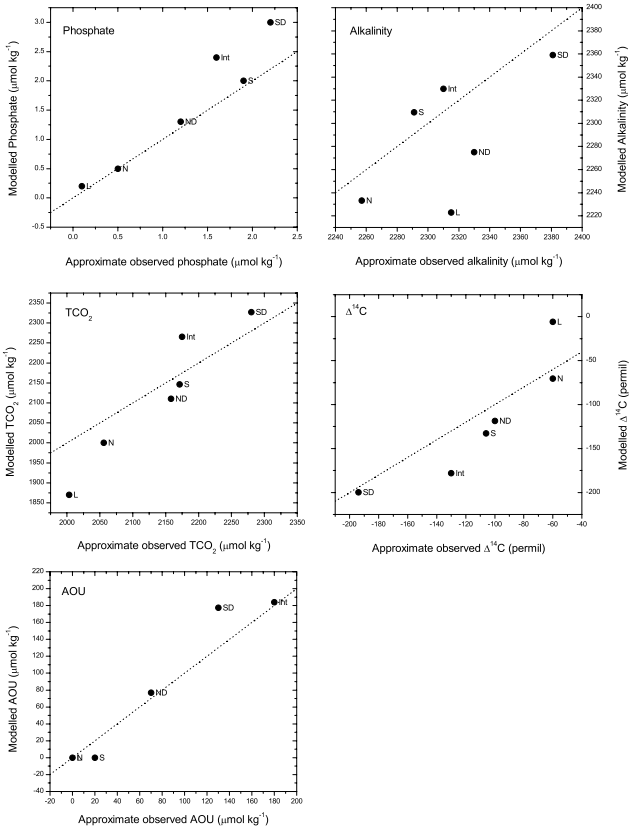


**Fig. 3.** Comparison of "baseline" box-model scenario results ($y$-axes) versus plausible expected values based on observations ($x$-axes; see text). The parameterisation used for the baseline model run is given in Table 1. Dotted lines indicate 1:1 relationship (i.e. equivalent modelled and expected values).

shoaled to a depth of ∼1.8 to 2.5 km, and was replaced at greater depths by southern-sourced (or LCDW-like) deep-water (Lynch-Steiglitz et al., 2007; Marchitto and Broecker, 2005; Hodell et al., 2003). New $\varepsilon_{Nd}$ evidence from the deep South Atlantic and Indian Ocean (Piotrowski et al., 2009; Piotrowski et al., 2008) also indicates a marked reduction in the contribution of NADW to LCDW exported to these basins.

If we take into account the hypsometry of the ocean floor (Menard and Smith, 1966), and if we assume that northern-sourced deep-water can account for up to 50% of the Lower Circumpolar Deep Water (LCDW) that is exported to the deep Indo-Pacific basins (Broecker and Peng, 1982; Matsumoto, 2007), then we can calculate the expected global volume ratio ($R_{ns}$) of "northern-sourced deep-water" (NDW) *versus* "southern-sourced deep-water" (SDW) given the depth of a presumed (horizontal) boundary between the two. The rationale behind this approach is that if NADW does not affect the Atlantic sector of the Southern Ocean below a given depth, then LCDW exported to the Indo-Pacific below this depth would also be without significant NADW influence. This is illustrated in Fig. 4, where a rise in the NDW/SDW boundary from 5 km to 2.5 km in the Atlantic is taken to imply a proportionate reduction of the amount of NDW mixed into the Indo-Pacific basins via CDW and hence a global reduction in the total volume ratio of northern- to southern deep-water ($R_{ns}$) from 1.43 to 0.5 between the Holocene and the LGM. Using more sophisticated models of the ocean circulation it should be possible to determine this ratio more exactly for a "physically sensible" ocean circulation and water-mass geometry (e.g. Cox, 1989). This could eventually permit a "calibration" of simulated changes in atmospheric $pCO_2$ to simulated changes in $R_{ns}$ (including perhaps for different causes of $R_{ns}$ change).

In the box model described here, equilibrium atmospheric $pCO_2$ is found to drop consistently as the $R_{ns}$ value for the box-model geometry decreases (i.e. NDW gives way

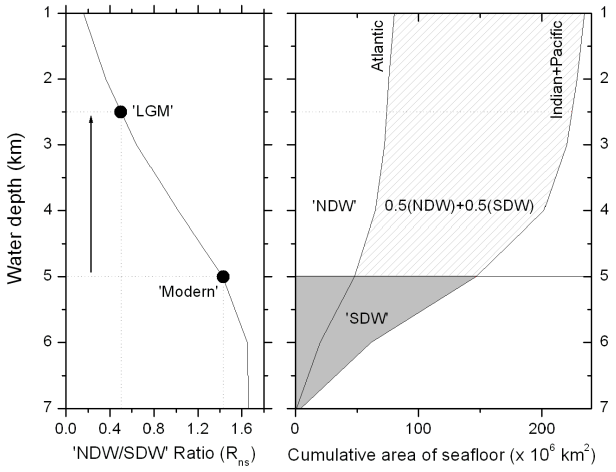


**Fig. 4.** Illustration of how the volume ratio ($R_{ns}$) of "northern" (NDW) to "southern" (SDW) water-masses is hypothesised to change based on water-mass boundary shoaling and given the hypsometry of the sea floor. The left hand panel shows changing water-mass ratio $R_{ns}$ versus the water depth of a presumed horizontal water-mass boundary. Solid dots indicate estimated values for "modern" and last glacial maximum (LGM) hydrography. The right hand panel shows how the sea floor area varies with water depth in the Atlantic and Indo-Pacific basins. Shading illustrates how $R_{ns}$ is calculated, by assuming that SDW fills the abyssal ocean up to the presumed water-mass boundary, while NDW fills only half of the Indo-Pacific basin and all of the Atlantic basin above this. The volume ratio $R_{ns}$ for a given fill depth is thus estimated as the volume above the fill depth in the Atlantic, plus half the volume above the fill depth in the Indo-Pacific, divided by the volume below the fill depth in the Atlantic and the Indo-Pacific plus half the volume above the fill depth in the Indo-Pacific. This tempers the exaggeration in volume change that would otherwise result from treating the whole ocean as analogous to the Atlantic.

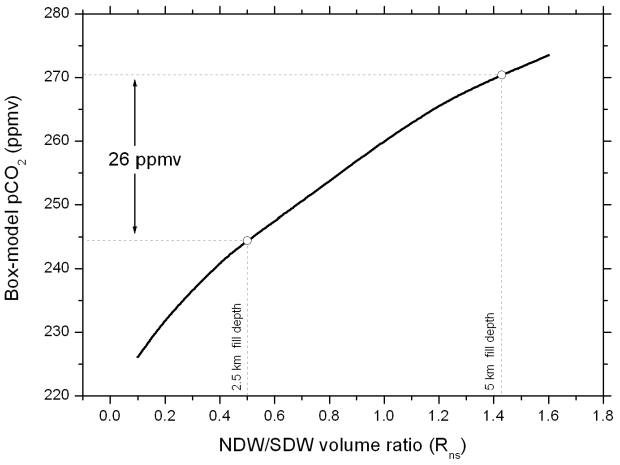


**Fig. 5.** Sensitivity of modelled atmospheric pCO2 to changes in the NDW/SDW volume ratio ($R_{ns}$). As the water-mass boundary shoals from 5 km (modern baseline) to 2.5 km (last glacial), $R_{ns}$ is estimated to change from 1.43 to 0.5. This results in a 26 ppm drop in atmospheric $pCO_2$ in the box model.

to SDW). This is shown in Fig. 5, where a shift in the NDW/SDW water-mass boundary from 5 km to 2.5 km (or a change in $R_{ns}$ from 1.43 to 0.5) corresponds to a drop in equilibrium atmospheric $pCO_2$ of just over 25 ppm. The box model volumes and chemical inventories for the hypothesised "glacial" water-mass geometry (2.5 km NDW/SDW water-mass boundary, $R_{ns}$=0.5) are summarised in Table 3. As expected, a "standing volume effect" such as described here is not going to account for the entirety of glacial-interglacial $pCO_2$ change. However, the important and perhaps surprising observation is that this mechanism might account for nearly as much of the glacial-interglacial atmospheric $pCO_2$ change as has been attributed to other fundamental mechanisms, such as sea-surface cooling, carbonate compensation, or ocean fertilisation (Sigman and Boyle, 2000; Peacock et al., 2006; Brovkin et al., 2007).

## 5 Discussion: sustaining a "standing volume" effect

The box model experiments illustrated in Fig. 5 appear to confirm the thought experiment described in Sect. 2.0, whereby an ocean that is dominated by LCDW-like deep water holds more $CO_2$. In order to operate effectively however, this sequestration mechanism requires three conditions: 1) there must be rather large changes in water-mass volumes (in the scenario envisaged here ∼60% of the Atlantic and ∼30% of the Indo-Pacific is affected by the reduced NADW contribution); 2) the expanding water-mass must have high $TCO_2$ relative to the water it effectively displaces; and 3) the expanding southern overturning loop must not "leak" $CO_2$ to the atmosphere very efficiently. These three conditions stem from the fact that the standing volume effect operates by causing an increase in the "efficiency" of the biological pump (via an increase in the deep sea nutrient pool), and by enhancing the solubility pump (via an expansion of a water-mass that is colder and relatively poorly equilibrated with the atmosphere), in both cases for a given overturning flux and polar outcrop area. If combined with a lower global average temperature, the expansion of a colder deep water-mass would further reduce the average ocean heat content. Once again, the key point is that a change in deep water-mass geometry could provide an effective means of keeping the ocean interior cold (against diffusive and geothermal warming from above and below), without any changes in overall overturning rates. This could be particularly important for enhancing the vertical abyssal temperature gradient if indeed the advection rate of cold deep-water from the poles was significantly reduced during the last glacial, relative to today.

**Table 3.** Box concentrations and inventories for "glacial" run ($R_{ns}$=0.5).

| $R_{ns}$=1.43 | | Box inventories | | | | Box inventories | | | |
|---|---|---|---|---|---|---|---|---|---|
| Box | Box inventory ($10^{19}$ kg) | $TCO_2$ ($\mu$mol kg$^{-1}$) | Alkalinity ($\mu$mol kg$^{-1}$) | $\Delta^{14}C$ (‰) | Phosphate ($\mu$mol kg$^{-1}$) | $TCO_2$ (mol) | Alkalinity (mol) | $^{14}C$ (mol) | Phosphate (mol) |
| South high latitude | 1.523 | 2114 | 2293 | −119 | 1.60 | 3.220E+16 | 3.493E+16 | 3.34E+04 | 2.437E+13 |
| Low latitude | 2.725 | 1842 | 2213 | 11 | 0.00 | 5.019E+16 | 6.030E+16 | 5.97E+04 | 0.000E+00 |
| North high latitude | 0.627 | 1967 | 2222 | −53 | 0.30 | 1.234E+16 | 1.393E+16 | 1.37E+04 | 1.881E+12 |
| North deep | 29.7 | 2071 | 2261 | −100 | 1.00 | 6.150E+17 | 6.715E+17 | 6.51E+05 | 2.970E+14 |
| Intermediate depth | 40.87 | 2224 | 2314 | −162 | 2.10 | 9.087E+17 | 9.456E+17 | 8.96E+05 | 8.583E+14 |
| South deep | 59.4 | 2303 | 2346 | −190 | 2.70 | 1.368E+18 | 1.394E+18 | 1.30E+06 | 1.604E+15 |
| Atmosphere | 1.77E+20 (mol) | 244 (ppm) | | 20.02 | | 4.333E+16 | | 5.20E+04 | |
| | | | | | Total inventories: | 3.03E+18 | 3.12E+18 | 3.01E+06 | 2.769E+15 |

Because the proposed standing volume effect operates via modulations of the biological and solubility pumps, it should combine additively with other imposed changes in gas-exchange or nutrient utilisation in the Southern Ocean, due to sea-ice expansion, increased upper-ocean stratification or ocean fertilisation for example. This is shown in Fig. 6, which shows that independently imposed changes in Southern Ocean air-sea gas exchange do not attenuate the standing volume effect at all, while a completely depleted Southern Ocean nutrient pool only attenuates the standing volume effect by ∼50% (due to the near elimination of the surface nutrient pool that the expanding SDW can draw from). One implication of the results shown in Fig. 6 is that imposed changes in gas exchange or biological export will result in a greater change in atmospheric $pCO_2$ if they are accompanied by an increase in the volumetric dominance of southern-sourced deep-water.

Previously, it has been suggested on the basis of first order principles and numerical modelling experiments that if global nutrient inventories are maintained while surface nutrients are depleted, either via reduced overturning rates or increased biological export rates, atmospheric $pCO_2$ will vary in proportion to the resulting average preformed nutrient concentration of the deep sea (Ito and Follows, 2005; Sigman and Haug, 2003; Toggweiler et al., 2003; Marinov et al., 2006). The average deep-sea preformed nutrient concentration is thus suggested to scale with atmospheic $pCO_2$, with an estimated ∼130–170 ppm change in $pCO_2$ per 1 $\mu$mol kg$^{-1}$ change in preformed phosphate (Ito and Follows, 2005; Sigman and Haug, 2003; Marinov et al., 2006). One way to explain the positive correlation is that any change that acts to reduce the mean nutrient (i.e. phosphate) concentration at the ocean surface (especially in regions of deepwater formation, Marinov et al., 2006) will result in: (1) a reduction of the advected nutrient flux into the ocean interior (thus lowering the mean preformed nutrient concentration of deep sea); and (2) an increase in the total nutrient concentration of the deep-sea (due to the conservation of ocean nutrients), thus sequestering more carbon in the deep sea.

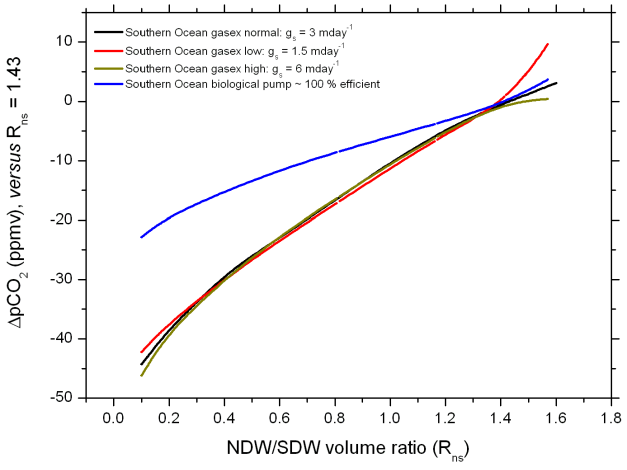


**Fig. 6.** Sensitivity of the modelled change in atmospheric $pCO_2$ to changes in $R_{ns}$ when Southern Ocean gas exchange efficiency is enhanced/reduced and Southern Ocean biological export efficiency is enhanced to 100%. The sensitivity of $pCO_2$ to $R_{ns}$ remains positive in each case, such that a reduction in $pCO_2$ driven by gas exchange or biological export change would be enhanced by a reduction in $R_{ns}$.

The proposed scaling between mean deep-sea preformed nutrient concentrations and atmospheric $pCO_2$ might be taken to imply that the domination of the deep sea by LCDW-like deep water (with a relatively high preformed nutrient concentration) would cause atmospheric $pCO_2$ to rise, contrary to the hypothesis presented here (Toggweiler et al.,

2003; Sigman and Haug, 2003). This apparent contradiction can be clarified by considering a heterogeneous deep-sea with constant total volume despite variable deep-sea water-mass volumes. The conservation of the global carbon inventory in this system can be stated as follows:

$$B_{\mathrm{tot}} = M\ p\mathrm{CO_2} + V_{\mathrm{surf}}\left\{\overline{C_{\mathrm{surf}}}\right\} + V_d\left\{\overline{C_d}\right\}$$
$$= M\ p\mathrm{CO_2} + V_{\mathrm{surf}}\left\{\overline{C_{\mathrm{surf}}}\right\} + V_{sd}\left\{C_{sd}\right\} + V_{nd}\left\{C_{nd}\right\}$$

where $M$ is the total molar content of the atmosphere; $V_d$, $V_{sd}$, $V_{nd}$ and $V_{\mathrm{surf}}$ are the volumes of the whole deep ocean, southern deep-water component, northern deep-water component, and surface ocean respectively; $\overline{C_d}$ and $\overline{C_{\mathrm{surf}}}$ are the mean carbon concentrations in the deep- and surface ocean; $C_{sd}$ and $C_{nd}$ are the southern- and northern deep-water carbon concentrations; and $B_{\mathrm{tot}}$ is the global carbon inventory. In this system, any perturbation to the carbon budget of the deep-sea must be balanced by a change in the atmospheric carbon content, which will remain in approximate equilibrium with the carbon content of the surface ocean. If we consider a perturbation to the system due only to changing $V_s$ at the expense of $V_n$ (i.e. $\delta V_{sd} = -\delta V_{nd}$), where $R_{C:P}$ is the Redfield $C{:}P$ ratio, then we find that (cf. Ito and Follows, 2005):

$$\frac{\delta p\mathrm{CO_2}}{\delta V_{sd}} = \frac{(C_{nd} - C_{sd})}{M\gamma} = \frac{R_{C:P}\,(P_{nd} - P_{sd})}{M\gamma} =$$
$$\frac{V_{\mathrm{surf}}\,R_{C:P}\,(\Delta P_{\mathrm{surf}})}{\delta V_{sd} M\gamma}$$

where:

$$\gamma = 1 + \frac{V_{\mathrm{surf}}\overline{C_{\mathrm{surf}}}}{M\gamma_{\mathrm{DIC}}\,p\mathrm{CO_2}}$$

In the above equation $\gamma$ is a dimensionless parameter that accounts for the equilibration between the atmosphere and the surface ocean, and represents the relative magnitudes of the atmospheric and surface ocean carbon reservoirs, via the "Revelle factor" (buffer factor), $\gamma_{\mathrm{DIC}}$. Although this parameter may vary with physical/climatic conditions, it is assumed to be constant in the discussion that follows. This is justified on the grounds that during the last glacial any changes in $\gamma$ are likely to have been negative rather than positive, as a result of decreased equilibration between the glacial ocean and the atmosphere, especially in the Southern Ocean as described in Sect. 2. This would only tend to exacerbate, rather than attenuate, the relationships described below.

The above relationships, which are drawn from the framework proposed by Ito and Follows (2005), confirm the intuitive expectation that changes in $p\mathrm{CO_2}$ and the surface nutrient concentration ($\Delta P_{\mathrm{surf}}$) or $\mathrm{TCO_2}$ should all be negative for increasing $V_s$ as long as the expanding southern deep-water mass has a higher nutrient content and $\mathrm{TCO_2}$ than the water-mass it replaces ($C_{sd} > C_{nd}$). Otherwise, the opposite is true. The mean preformed nutrient concentration of the deep sea can be defined as the total flux of dissolved nutrients into the sub-surface (i.e. the sum of the products of surface phosphate and their associated downward mass transport terms) divided by the net overturning circulation (e.g. Sigman and Haug, 2003). This means that mean preformed nutrients in the deep-sea must also decrease as $V_{sd}$ increases and $p\mathrm{CO_2}$ decreases (again if $C_{nd} < C_{sd}$). Hence as long as the postulated changes in deep water-mass volumes cause the surface $\mathrm{TCO_2}$ and nutrient concentrations to drop (especially in regions of deep-water formation), we can expect them to cause a drop in atmospheric $p\mathrm{CO_2}$ and a drop in mean deep-water preformed nutrient concentration, all because of an increase in the total deep-sea nutrient *inventory*.

In the box model experiments carried out here, the expected theoretical relationships based on the arguments presented above, and based on previous work (Ito and Follows, 2005; Sigman and Haug, 2003; Toggweiler et al., 2003; Marinov et al., 2006), are borne out: atmospheric $p\mathrm{CO_2}$ drops by almost 100 ppm per 1 $\mu$mol kg$^{-1}$ drop in the mean preformed nutrient concentration in the ocean interior boxes (calculated from Tables 1, 2 and 3). The proposed standing volume effect therefore appears to be consistent with previous conceptualisations of the biological pump and its variable efficiency, although it demonstrates that dissolved- or particulate export rates are not the only parameters controlling the mean surface-to-deep nutrient/carbon concentration gradient in a closed system.

## 6 Ocean circulation and the "$CO_2$ stew"

The main purpose of the present study is not to attempt a complete simulation or explanation of glacial-interglacial atmospheric $CO_2$ change, nor is it to suggest that ocean circulation rates and biological export rates are unimportant for glacial-interglacial $CO_2$ change. Rather, the goal here is to draw a distinction between two separate aspects of the "ocean circulation" (water-mass distribution *versus* water-mass renewal/overturning rates) in terms of their respective roles in glacial-interglacial $CO_2$ change. Based on a simple thought experiment and a set of box-model tests, it would appear that a surprisingly large portion of the glacial-interglacial $CO_2$ change might be explained simply by changes in the volumetric contribution of contrasting deep-water end-members to the deep sea, prior to any imposed changes in overturning-, gas exchange- or biological export rates. The proposed "standing volume effect" would arise due to substantial changes in the volume of relatively high-$\mathrm{TCO_2}$ (LCDW-like) deep-water filling the ocean basins, and requires only that the expanding overturning loop does not "leak" excess $CO_2$ to the atmosphere as a result of countervailing changes in biological export rates or gas exchange rates for example. Indeed, the standing volume effect

will be additive with respect to accompanying changes in biological export or gas exchange around Antarctica.

Although previous studies that have simulated glacial atmospheric $CO_2$ using complex numerical models with accurate bathymetry (e.g. Heinze et al., 1991) may have already included the proposed standing volume effect implicitly, none so far have tried to identify or quantify its possible impact on glacial $CO_2$ draw-down. Although one recent exception (Brovkin et al., 2007) has suggested that the expansion of AABW at the expense of NADW in the glacial ocean might have caused atmospheric $CO_2$ to drop by as much as 43 ppm, this estimate includes the effects of changes in deep-water overturning rates (reduced NADW export rate by ∼20% and intensified AABW export rate). The proposed standing volume effect therefore remains to be tested adequately using complex numerical model simulations of the glacial ocean circulation.

If the simple standing volume mechanism proposed here for enhancing deep-sea carbon sequestration can be incorporated into the list of "ingredients" that have contributed to glacial-interglacial $CO_2$ change (Peacock et al., 2006; Kohler et al., 2005; Archer et al., 2000; Sigman and Boyle, 2000), it may help to reduce or eliminate the $CO_2$ deficit that remains to be explained by appealing to more equivocal or controversial processes. More importantly however, it may also help us to evaluate more explicitly the role of the 'ocean circulation' as an ingredient in the glacial-interglacial "$CO_2$ stew", as well as the triggers that repeatedly pushed the marine carbon cycle between glacial and interglacial modes (Paillard and Parrenin, 2004; Shackleton, 2000). This is especially true if the mechanisms or timescales for changing the vertical mass transport rate in the ocean differ from those for changing the (vertical) redistribution of contrasting deep-water end-members. Indeed, a de-convolution of the expected impacts of an altered "ocean circulation" into renewal-rate effects and standing-volume effects can only gain importance to the extent that proxy evidence for a large reduction in the net overturning rate of the glacial ocean remains equivocal (Lynch-Steiglitz et al., 2007), and/or theoretical support for such a change continues to be debated (Wunsch, 2003).

*Acknowledgements.* The author is grateful for helpful discussions with E. Gloor, P. Koelher, R. Toggweiler, E. Galbraith and M. McIntyre, as well as the input of two anonymous reviewers. The author would also like to acknowledge research fellowships provided by The Royal Society and Christ's College Cambridge.

Edited by: R. Zeebe

## References

Adkins, J. F., McIntyre, K., and Schrag, D. P.: The salinity, temperature and d18o of the glacial deep ocean, Science, 298, 1769–1773, 2002.

Archer, D. and Maier-Reimer, E.: Effect of deep-sea sedimentary calcite preservation on atmospheric co$_2$ concentration, Nature, 367, 260–263, 1994.

Archer, D., Winguth, A., Lea, D. W., and Mahowald, N.: What caused the glacial/interglacial atmospheric $pco_2$ cycles?, Rev. Geophys., 38, 159–189, 2000.

Bard, E.: Correction of accelerator mass spectrometry 14c ages measured in planktonic foraminifera: Paleoceanographic implications, Paleoceanography, 3, 635–645, 1988.

Barker, S., Diz, P., Vautravers, M., Pike, J., Knorr, G., Hall, I. R., and Broecker, W.: Interhemispheric atlantic seesaw response during the last deglaciation, Nature, 457, 1097–1102, 2009.

Boyle, E.: Cadmium and d13c paleochemical ocean distributions during the stage 2 glacial maximum, Ann. Rev. Earth Planet. Sci., 20, 245–287, 1992.

Boyle, E. A.: The role of vertical fractionation in controlling late quaternary atmospheric carbon dioxide, J. Geophys. Res., 93, 15701–715714, 1988a.

Boyle, E. A.: Cadmium: Chemical tracer fro deepwater paleoceanography, Paleoceanography, 3, 471–489, 1988b.

Broecker, W. S.: Glacial to interglacial changes in ocean chemistry, Prog. Oceanogr., 11, 151–197, 1982a.

Broecker, W. S.: Ocean chemistry during glacial time, Geochim. Cosmochim. Ac., 46, 1698–1705, 1982b.

Broecker, W. S. and Peng, T. H.: Tracers in the sea, Eldigio Press, Palisades, New York, USA, 690 pp., 1982.

Broecker, W. S. and Peng, T.-H.: The cause of the glacial to interglacial atmospheric co$_2$ change: A polar alkalinity hypothesis, Global Biogeochem. Cy., 3, 215–239, 1989.

Brovkin, V., Ganopolski, A., Archer, D., and Rahmstorf, S.: Lowering glacial atmospheric co$_2$ in response to changes in oceanic circulation and marien biogeochemistry, Paleoceanography, 22, 1–14, 2007.

Cox, M. D.: An idealized model of the world ocean. Part i: The global-scale water masses, J. Phys. Oceanogr., 19, 1730–1752, 1989.

Curry, W. B., Duplessy, J. C., Labeyrie, L. D., and Shackleton, N. J.: Changes in the distribution of d13c of deep water sigma-co$_2$ between the last glaciation and the holocene, Paleoceanography, 3, 317–341, 1988.

Curry, W. B. and Oppo, D. W.: Glacial water mass geometry and the distribution of $\delta^{13}C$ of sigma-$CO_2$ in the western atlantic ocean, Paleoceanography, 20, PA1017, doi:10.1029/2004PA001021,2005.

Denman, K. L., Brasseur, G., Chidthaisong, A., Ciasis, P., Cox, P. M., Dickinson, R. E., Hauglustaine, D., Heinze, C., Holland, E., Jacob, D., Lohmann, U., Ramachandran, S., da Silva Dias, P. L., Wofsy, S. C., and Zhang, X.: Couplings between changes in the climate system and biogeochemistry, in: Climate change 2007: The physical basis. Contribution of working group i to the fourth assessment report of the intergovernmental panel on climate change, edited by: Solomon, S., Qin, D., Manning, M., Chen, Z., Marquis, M., Averyt, K. B., Tignor, M., and Miller, H. L., Cambridge University Press, Cambridge, New York, 499–587, 2007.

Dugdale, R. C.: Nutrient limitation in the sea: Dynamics, identification, and significance, Limnol. Oceanogr., 12, 685–695, 1967.

Duplessy, J.-C., Shackleton, N. J., Fairbanks, R. G., Labeyrie, L., Oppo, D., and Kallel, N.: Deep water source variations during

the last climatic cycle and their impact on global deep water circulation, Paleoceanography, 3, 343–360, 1988.

Ganachaud, A. and Wunsch, C.: Improved estimates of global ocean circulation, heat transport and mixing from hydrographic data, Nature, 408, 453–457, 2000.

Garcia, H. E., Locarnini, T. P., and Antonov, J. I.: World ocean atlas 2005, volume 4, Nutrients (phosphate, nitrate, silicate), US Government Printing Office, Washington DC, USA, 396 pp., 2006.

Gildor, H. and Tziperman, E.: Physical mechanisms behind biogeochemical glacial-interglacial $co_2$variations, Geophys. Res. Lett., 28, 2421–2424, 2001.

Gnanadesikan, A., de Boer, A. M., and Mignone, B. K.: A simple theory of the pycnocline and overturning revisited, in: Ocean circulation: Mechanisms and impacts, edited by: Schmittner, A., Chiang, C. H., and Hemming, S. R., Geophysical monograph, AGU, Washington DC, USA, 19–32, 2007.

Goldstein, S. L. and Hemming, S. R.: Long-lived isotopic tracers in oceanography, paleoceanography and ice-sheet dynamics, in: Treatise on geochemistry, edited by: Elderfield, H., Elsevier, 453–489, 2003.

Gordon, A. L.: Comment on the south atlantic's role in the global circulation, in: The south atlantic: Present and past circulation, edited by: Wefer, G., Berger, A., Siedler, G., and Webb, D. J., Springer-Verlag, Berlin, Heidelberg, Germany, 121–124, 1996.

Heinze, C., Maier-Reimer, E., and Winn, K.: Glacial $pco_2$ reduction by the world ocean: Experiments with the hamburg carbon cycle model, Paleoceanography, 6, 395–430, 1991.

Hodell, D. A., Venz, K. A., Charles, C. D., and Ninneman, U. S.: Pleistocene vertical carbon isotope and carbonate gradients in the south atlantic sector of the southern ocean, Geochem. Geophys. Geosys., 4, GC1004, doi:10.1029/2002GC000367, 2003.

Ito, T. and Follows, M. J.: Preformed phosphate, soft tissue pump and atmospheric $co_2$, J. Mar. Res., 63, 813–839, 2005.

Keeling, R. F. and Stephens, B. B.: Antarctic sea ice and the control of pleistocene climate instability, Paleoceanography, 16, 112–131, 2001.

Keigwin, L. D. and Lehmann, S. J.: Deep circulation change linked to heinrich event 1 and younger dryas in a mid-depth north atlantic core, Paleoceanography, 9, 185–194, 1994.

Keigwin, L. D.: Radiocarbon and stable isotope constraints on last glacial maximum and younger dryas ventilation in the western north atlantic, Paleoceanography, 19, 1–15, 2004.

Key, R. M., Kozyr, A., Sabine, C., Lee, K., Wanninkhof, R., Bullister, J. L., Feely, R. A., Millero, F. J., Mordy, C., and Peng, T.-H.: A global ocean carbon climatology: Results from the global data analysis project (glodap), Global Biogeochem. Cycles, 18, 1–23, 2004.

Kim, S.-J., Flato, G. M., and Boer, G. J.: A coupled climate model simulation of the last glacial maximum, part 2: Approach to equilibrium, Clim. Dynam., 20, 635–661, 2003.

Knox, F. and McElroy, M.: Changes in atmospheric $co_2$: Influence of marine biota at high latitude, J. Geophys. Res., 89, 4629–4637, 1984.

Kohler, P., Fischer, H., Munhoven, G., and Zeebe, R. E.: Quantitative interpretation of atmospheric carbon records over the last glacial termination, Global Biogeochem. Cy., 19, 1–24, 2005.

Lynch-Steiglitz, J., Adkins, J. F., Curry, W. B., Dokken, T., Hall, I. R., Heguera, J. C., Hirschi, J. J.-M., Ivanova, E. V., Kissel, C., Marchal, O., Marchitto, T. M., McCave, I. N., McManus, J. F., Mulitza, S., Ninneman, U. S., Peeters, F. J. C., Yu, E.-F., and Zahn, R.: Atlantic meridional overturning circulation during the last glacial maximum, Science, 316, 66–69, 2007.

Marchal, O., Stocker, T. F., and Joos, F.: A latitude-depth, circulation-biochemical ocean model for paleoclimate studies. Development and sensitivities, Tellus, 50B, 290–316, 1998.

Marchal, O. and Curry, W. B.: On the abyssal circulation in the glacial atlantic, J. Phys. Oceanogr., 38, 2014–2037, 2008.

Marchitto, T. M., Oppo, D. W., and Curry, W. B.: Paired benthic foraminiferal cd/ca and zn/ca evidence for a greatly increased presence of southern ocean water in the glacial north atlantic, Paleoceanography, 17, 10.11–10.16, 2002.

Marchitto, T. M. and Broecker, W.: Deep water mass geometry in the glacial atlantic ocean: A review of constraints from the paleonutrient proxy cd/ca, Geochem. Geophys. Geosys., 7, 1–16, 2005.

Marchitto, T. M., Lehman, S. J., Otiz, J. D., Fluckiger, J., and van Geen, A.: Marine radiocarbon evidence for the mechanism of deglacial atmospheric $co_2$ rise, Science, 316, 1456–1459, 2007.

Marinov, I., Gnadesikan, A., Toggweiler, J. R., and Sarmiento, J. L.: The southern ocean biogeochemical divide, Nature, 441, 964–967, 2006.

Martin, J. H., Knauer, G. A., Karl, D. M., and Broenkow, W. W.: Vertex: Carbon cycling in the northeast pacific, Deep-Sea Res., 34, 267–286, 1987.

Matsumoto, K.: Radiocarbon-based circulation age of the world oceans, J. Geophys. Res., 112, 1–7, 2007.

Menard, H. W. and Smith, S. M.: Hypsometry of ocean basin provinces, J. Geophys. Res., 71, 4305–4325, 1966.

Michel, E., Labeyrie, L., Duplessy, J.-C., and Gorfti, N.: Could deep subantarctic convection feed the worl deep basins during last glacial maximum?, Paleoceanography, 10, 927–942, 1995.

Millero, F. J.: Thermodynamics of the carbon dioxide system in the oceans, Geochim. Cosmochim. Ac., 59, 661–677, 1995.

Müller, S. A., Joos, F., Edwards, N. R., and Stocker, T. F.: Water mass distribution and ventilation time scales in a cost-efficient, three-dimensional ocena model, J. Climate, 19, 5479–5499, 2006.

Najjar, R. G., Sarmiento, J. L., and Toggweiler, J. R.: Downward transport and fate of organic matter in the ocean: Simulations with a general circulation model, Global Biogeochem. Cy. , 6, 45–76, 1992.

Naviera Garabato, A. C., Polzin, K. L., King, B. A., Heywood, K. J., and Visbeck, M.: Widespread intense turbulent mixing in the southern ocean, Science, 303, 210–213, 2004.

Ninneman, U. S. and Charles, C. D.: Changes in the mode of southern ocean circulation over the last glacial cycle revealed by foraminiferal stable isotopic variability, Earth Planet. Sci. Lett., 201, 383–396, 2002.

Oppo, D. and Fairbanks, R. G.: Atlantic ocean thermohaline circulation of the last 150 000 years: Relationship to climate and atmospheric $co_2$, Paleoceanography, 5, 277–288, 1990.

Oppo, D. W., Fairbanks, R. G., Gordon, A. L., and Shackleton, N. J.: Late pleistocene southern ocean $d^{13}c$ variability, Paleoceanography, 5, 43–54, 1990.

Orsi, A. H., Johnson, G. C., and Bullister, J. L.: Circulation, mixing and production of antarctic bottom water, Prog. Oceanogr., 43, 55–109, 1999.

Paillard, D. and Parrenin, F.: The antarctic ice sheet and the trig-

gering of deglaciations, Earth Planet. Sci. Lett., 227, 263–271, 2004.

Peacock, S., Lane, E., and Restrepo, M.: A possible sequence of events for the generalized glacial-interglacial cycle, Global Biogeochem. Cy., 20, 1–17, 2006.

Piotrowski, A., Goldstein, S. L., Hemming, S. R., and Fairbanks, R. G.: Temporal relationships of carbon cycling and ocean circulation at glacial boundaries, Science, 307, 1933–1938, 2005.

Piotrowski, A. M., Goldstein, S. L., Hemming, S. R., and Fairbanks, R. G.: Intensification and variability of ocean thermohaline circulation through the last deglaciation, Earth Planet. Sci. Lett., 225, 205–220, 2004.

Piotrowski, A. M., Goldstein, S. L., Hemming, S. R., Fairbanks, R. G., and Zylberberg, D. R.: Oscillating glacial northern and southern deep water formation from combined neodymium and carbon isotopes, Earth Planet. Sci. Lett., 272, 394–405, 2008.

Piotrowski, A. M., Banakar, V. K., Scrivner, A., Elderfield, H., Galy, A., and Dennis, A.: Indian ocean circulation and productivity during hte last glacial cycle, Earth Planet. Sci. Lett., 285, 179–189, 2009.

Redfield, A. C., Ketchum, B. H., and Richards, F. A.: The influence of organisms on the composition of sea water, in: The sea, edited by: Hill, M. N., Wiley-Interscience, New York, USA, 26–77, 1962.

Robinson, L. F., Adkins, J. F., Keigwin, L. D., Southon, J., Fernandez, D. P., Wang, S.-L., and Scheirer, D. S.: Radiocarbon variability in the western north atlantic during the last deglaciation, Science, 310, 1469–1473, 2005.

Rutberg, R. L., Heming, S. R., and Goldstein, S. L.: Reduced north atlantic deep water flux to the glacial southern ocean inferred from neodymium isotope ratios, Nature, 405, 935–938, 2000.

Sabine, C., Feely, R. A., Gruber, N., Key, R. M., Lee, K., Bullister, J. L., Wanninkhof, R., Wong, C. S., Wallace, D. W. R., Tilbrook, B., Millero, F. J., Peng, T.-H., Kozyr, A., Ono, T., and Rios, A. F.: The oceanic sink for anthropogenic $co_2$, Science, 305, 367–371, 2004.

Sarmiento, J. L. and Toggweiler, R.: A new model for the role of the oceans in determining atmospheric $pco_2$, Nature, 308, 621–624, 1984.

Schulz, M., Seidov, D., Sarnthein, M., and Stattegger, K.: Modeling ocean-atmosphere carbon budgets during the last glacial maximum-heinrich 1 meltwater event-bolling transition, Int. J. Earth Sci. (Geol Rundsch), 90, 412–425, 2001.

Shackleton, N. J.: The 100,000-year ice-age cycle identified and found to lag temperature, carbon dioxide and orbital eccentricity., Science, 289, 1897–1902, 2000.

Shin, S. I., Liu, Z., Otto-Bliesner, B. L., Brady, E. C., Kutzbach, J. E., and Harrison, S. P.: A simulation of the last glacial maximumclimate using the ncar-ccsm, Clim. Dynam., 20, 127–151, 2003.

Siegenthaler, U. and Wenk, T.: Rapid atmospheric $co_2$ variations and ocean circulation, Nature, 308, 624–625, 1984.

Siegenthaler, U., Stocker, T. F., Monnin, E., Luthi, D., Schwander, J., Stauffer, B., Raynaud, D., Barnola, J.-M., Fischer, H., Masson-Delmotte, V., and Jouzel, J.: Stable carbon cycle - climate relationship during the late pleistocene, Science, 310, 1313–1317, 2005.

Sigman, D. M. and Boyle, E. A.: Glacial/interglacial variations in atmospheric carbon dioxide, Nature, 407, 859–869, 2000.

Sigman, D. M. and Haug, G. H.: The biological pump in the past, in: Treatise on geochemistry, edited by: Elderfield, H., Elsevier, 491–528, 2003.

Skinner, L. C. and Shackleton, N. J.: Rapid transient changes in northeast atlantic deep-water ventilation-age across termination i, Paleoceanography, 19, 1–11, 2004.

Sloyan, B. and Rintoul, S. R.: The southern limb of the global overturning circulation, J. Phys. Oceanogr., 31, 143–173, 2001.

Speer, K., Rintoul, S. R., and Sloyan, B.: The diabatic deacon cell, J. Phys. Oceanogr., 30, 3212–3222, 2000.

Stuiver, M. and Polach, H. A.: Reporting of 14C data, Radiocarbon, 19, 355–363, 1977.

Toggweiler, J. R., and Sarmiento, J. L.: Glacial to interglacial changes in atmospheric carbon dioxide: The critical role of ocean surface water in high latitudes, in: The carbon cycle and atmospheric $co_2$: Natural variations archean to present, Geophysical monograph, American Geophysical Union, 163–184, 1985.

Toggweiler, J. R.: Variation of atmospheric $co_2$ by ventilation of the ocean's deepest water, Paleoceanography, 14, 571–588, 1999.

Toggweiler, J. R., Murnane, R., Carson, S., Gnanadesikan, A., and Sarmiento, J. L.: Representation of the carbon cycle in box models and gcms: 2. Organic pump, Global Biogeochem. Cy., 17, 27.21–27.13, 2003.

Tziperman, E. and Gildor, H.: On the mid-pleistocene transition to 100-kyr glacial cycles and the asymmetry between glaciation and deglaciation times, Paleoceanography, 18, PA1001, doi:10.1029/2001PA000627, 2003.

Watson, A. J. and Naveira Garabato, A. C.: The role of southern ocean mixing and upwelling in glacial-interglacial atmospheric $co_2$ change, Tellus, 58B, 73–87, 2006.

Webb, D. J. and Suginohara, N.: Vertical mixing in the ocean, Nature, 409, 37 pp., 2001, 2001.

Wunsch, C.: Determining paleoceanographic circulations, with emphasis on the last glacial maximum, Quat. Sci. Rev., 22, 371–385, 2003.

Yu, J. and Elderfield, H.: Benthic foraminiferal b/ca ratios reflect deep water carbonate saturation state, Earth Planet. Sci. Lett., 258, 73–86, 2007.

Zeebe, R. E. and Wolf-Gladrow, D.: $Co_2$ in seawater: Equilibrium, kinetics, isotopes, Elsevier oceanography series, Elsevier, Amsterdam NL, 2001.